Probing The Axion-Electron and Axion-Photon Couplings with the QUAX Haloscopes

Lab @INFN-**LNL**
C. Braggio (this presentation), **G. Carugno** (lead), A. Ortolan, G. Ruoso
A. Lombardi, R. Pengo, L. Taffarello
PhD+PostDoc (2017-2020): N. Crescini
PhD (2018-2020): R. Di Vora

100 μW at 100 mK

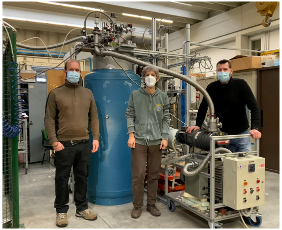

1 mW at 100 mK

Lab @INFN-**LNF**
C. Gatti, D. Alesini, D. Babusci, D. Di Gioacchino, C.Ligi, G. Maccarrone, D. Morricciani, S. Tocci
PhD (2018-2020): A. Rettaroli

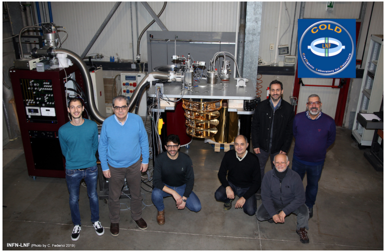

@INFN-**Salerno**
U. Gambardella, G. Iannone, C. Severino, D. D'Agostino
@INFN-**Trento**
P. Falferi, R. Mezzena

HALOSCOPE - resonant search for axion DM in the Galactic halo

– original proposal by P. Sikivie (1983)

– search for axions as cold dark matter constituent: SHM from Λ_{CDM}, local DM density ρ

$\rightarrow$ signal is a **line** with 10^{-6} relative width in the energy($\rightarrow$ frequency) spectrum

$\rightarrow$ + sharp (10^{-11}) components due to non-thermalized

– an **axion** may interact with a **strong** $\vec{B}$ **field** to produce a **photon** of a specific frequency ($\rightarrow m_a$)

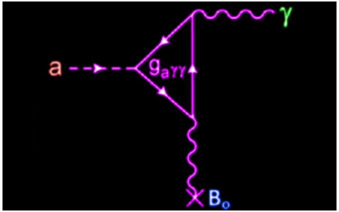

HALOSCOPE - resonant search for axion DM in the Galactic halo

— if axions are *almost monochromatic* then their conversion to detectable particles (photons) can be accomplished using *high-Q* microwave cavities.

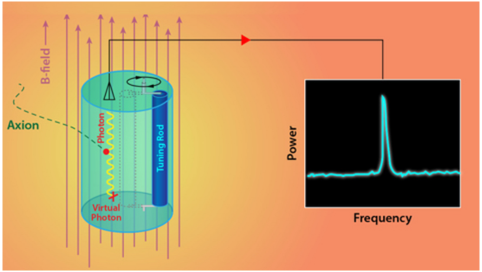

- $\omega_{\mathrm{TM}0nl} = \sqrt{\left(\frac{\epsilon_n}{r}\right)^2 + \left(\frac{l\pi}{h}\right)}$
  TM_{0nl} are the cavity modes that couple with the axion
- resonant amplification in $[m_a \pm m_a/Q]$
- data in thin slices of parameter space; typically $Q < Q_a \sim 1/\sigma_v^2 \sim 10^6$
- signal power $P_{a\to\gamma}$ is model-dependent

$$P_{a\to\gamma} \propto (B^2 VQ)(g_{a\gamma}^2 \frac{\rho}{m_a})$$

exceedingly tiny ($\sim 10^{-23}$ W)

"The last signal ever received from the 7.5 W transmitter aboard Pioneer 10 in 2002, then 12.1 billion kilometers from Earth, was a prodigious 2.5×10^{-21} *W. And unlike with the axion, physicists knew its frequency!"*

K. V. Bibber and L. Rosenberg, Physics Today 59, 8, 30 (2006)

HALOSCOPES: 2020 RESULTS

ADMX PRL **124**, 101303 (2020)

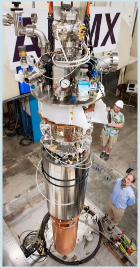

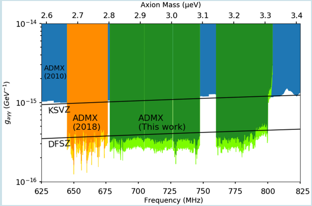

– sensitivity to QCD axion

– 2.82 – 3.31 μeV mass range

– cylindrical cavity at $T = 100\,$mK, $Q_0 \sim 30000$, $V = 136\,$l

– 7.6 T field

HAYSTAC arXiv:2008.01853 (2020)

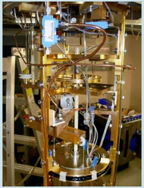

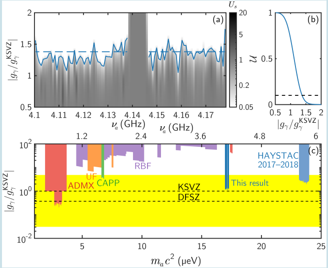

– 17.14 – 17.28 μeV axion mass range

– **squeezing** doubled the search rate

– cylindrical cavity at $T = 60\,$mK $Q_0 \sim 50000$, $V = 1.5\,$l

– 8T magnet

"Roberto and I spent a few months cooking up this theory, and now the experimentalists have spent 40 years looking for it "

H. Quinn

Haloscopes: 2020 results

CAPP
South Korea Institute

PRL 124, 101802 (2020)
PRL **125**, 221302 (2020)

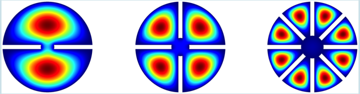

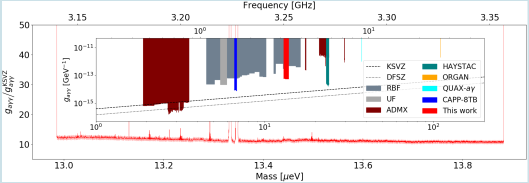

— multi-cell
— powerful magnets
— tailored cavities for high frequency

"Roberto and I spent a few months cooking up this theory, and now the experimentalists have spent 40 years looking for it"
H. Quinn

HALOSCOPES: DEMONSTRATORS AND NEW PROPOSALS

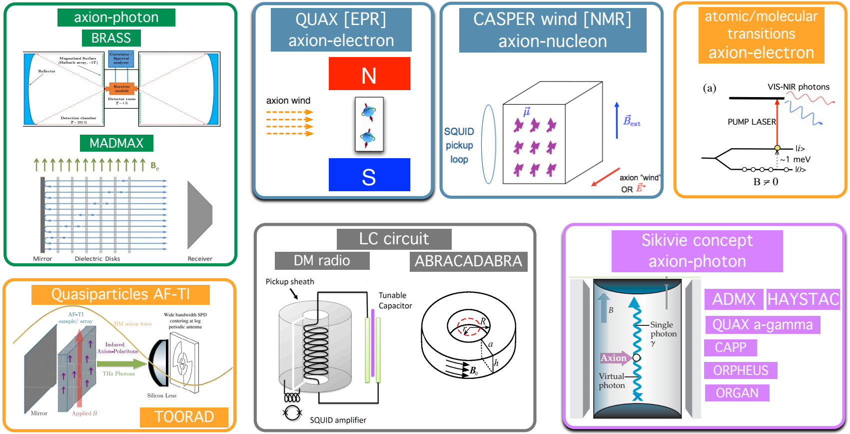

only a selection...

QUAX - QUAERERE AXIONS

Detection of cosmological axions through their **coupling to electrons** or **photons**

ELECTRON COUPLING – **QUAX** *the FMR haloscope*

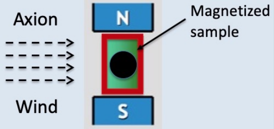

the axion DM cloud acts as an **effective RF magnetic field** on the electron spin exciting **magnetic transitions** in a magnetized sample (YIG) → **RF photons**

$$P_{\rm out} = \frac{P_{\rm in}}{2} = 8 \times 10^{-26} \left(\frac{m_a}{2 \cdot 10^{-4}\,{\rm eV}}\right)^3 \left(\frac{V_s}{1\ {\rm liter}}\right) \left(\frac{n_S}{10^{28}/{\rm m}^3}\right) \left(\frac{\tau_{\rm min}}{10^{-6}\,{\rm s}}\right)\ {\rm W},$$

PHOTON COUPLING – **QUAX** aγ *high frequency range* (8.5 — 11) GHz

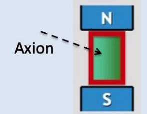

DM axions are converted into **RF photons** inside a **resonant cavity** immersed in a **strong magnetic field**

$$P_{\rm ax} = 3.3 \cdot 10^{-24}\,{\rm W} \left(\frac{V_{\rm eff}^{\rm Sa}}{2.3 \cdot 10^{-5}\,{\rm m}^3}\right) \left(\frac{B}{8\,{\rm T}}\right)^2 \times \left(\frac{g_\gamma}{-0.97}\right)^2 \left(\frac{\rho_a}{0.45\,{\rm GeV\,cm}^{-3}}\right) \left(\frac{f}{13.5\,{\rm GHz}}\right) \left(\frac{Q_L}{145\,000}\right)$$

AXIONS AND MAGNONS

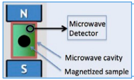

R. Barbieri et al.,
Searching for galactic axions through magnetized media: The QUAX proposal
Phys. Dark Univ. 15, 135 - 141 (2017)

1985 1990 2020

L1 L2

L. M. Krauss, J. Moody, **F. Wilczek**, D.E. Morris,
Calculations for cosmic axion detection,
Phys. Rev. Lett. 55, (1985)

R. Barbieri, M. Cerdonio, G. Fiorentini, S. Vitale,
Axion to magnon conversion, a scheme for detection of galactic axions
Phys. Lett. B **226**, 357 (1989)

F. Caspers, Y. Semertzidis,
Ferri-magnetic resonance, magnetostatic waves and open resonators for axion detection
Workshop on Cosmic Axions, World Scientific Pub. Co., Singapore, p. 173 (1990)

A.I. Kakhizde, **I.V. Kolokolov**,
Antiferromagnetic axion detector
Sov. Phys, JETP **72** 598 (1991)

Detecting Light Dark Matter with Magnons
T. Trickle, Z. Zhang, and K. M. Zurek
Phys. Rev. Lett. 124, 201801 (2020)

So Chigusa, T. Moroi, and K. Nakayama,
Detecting light boson dark matter through conversion into a magnon
Phys. Rev. D 101, 096013 (2020)

G. Flower *et al*
Broadening frequency range of a FMR axion haloscope with strongly coupled cavity-magnon polaritons
Phys. Dark Univ. 25, 100306 (2019)

AXIONS AND MAGNONS

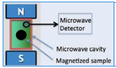

R. Barbieri et al.,
Searching for galactic axions through magnetized media: The QUAX proposal
Phys. Dark Univ. 15, 135 - 141 (2017)

L. M. Krauss, J. Moody, **F. Wilczek**, D.E. Morris,
Calculations for cosmic axion detection,
Phys. Rev. Lett. 55, (1985)

R. Barbieri, M. Cerdonio, G. Fiorentini, S. Vitale,
Axion to magnon conversion, a scheme for detection of galactic axions
Phys. Lett. B **226**, 357 (1989)

F. Caspers, Y. Semertzidis,
Ferri-magnetic resonance, magnetostatic waves and open resonators for axion detection
Workshop on Cosmic Axions, World Scientific Pub. Co., Singapore, p. 173 (1990)

A.I. Kakhizde, **I.V. Kolokolov**,
Antiferromagnetic axion detector
Sov. Phys, JETP **72** 598 (1991)

Detecting Light Dark Matter with Magnons
T. Trickle, Z. Zhang, and K. M. Zurek
Phys. Rev. Lett. 124, 201801 (2020)

So Chigusa, T. Moroi, and K. Nakayama,
Detecting light boson dark matter through conversion into a magnon
Phys. Rev. D 101, 096013 (2020)

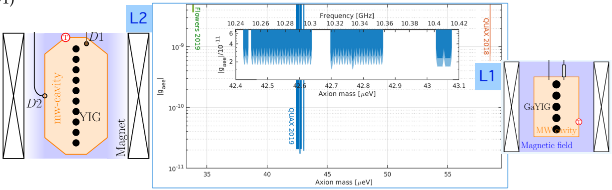

Interaction of the axion with a spin 1/2 particle

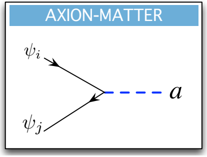

$$\mathcal{L}_a = f_a^{-1} g_{aij} \bar{\psi}_i \gamma^\mu \gamma^5 \psi_j \partial_\mu a$$

DFSZ axion model coupling with non relativistic ($v/c \ll 1$) electron: equation of motion reduces to

$$i\hbar \frac{\partial \varphi}{\partial t} = \left[-\frac{\hbar^2}{2m} \nabla^2 - \frac{g_p \hbar}{2m} \boldsymbol{\sigma} \cdot \boldsymbol{\nabla} a \right] \varphi$$

The interaction term is in the form of a spin−magnetic field interaction with ∇a playing the role of a oscillating effective magnetic field

$$-\frac{g_p \hbar}{2m} \boldsymbol{\sigma} \cdot \boldsymbol{\nabla} a \equiv -2 \frac{e\hbar}{2m} \boldsymbol{\sigma} \cdot \left(\frac{g_p}{2e} \right) \boldsymbol{\nabla} a$$

$-2\mu_B \boldsymbol{\sigma}$,

μ_B the Bohr magneton

$$B_a \equiv \frac{g_p}{2e} \boldsymbol{\nabla} a$$

effective magnetic field

QUAX: AXION DETECTION BY RESONANT INTERACTION WITH e^- SPIN

The interaction term has the form of a spin—magnetic field interaction with ∇a playing the role of a

oscillating effective magnetic field

$$\frac{\omega_a}{2\pi} = f_a = \frac{m_a c^2}{h} \simeq 14 \left(\frac{m_a}{58.5\,\mu\text{eV}}\right) \text{GHz},$$

$$\underbrace{B_a \equiv \frac{g_p}{2e} \nabla a}_{\text{effective magnetic field}} \longrightarrow B_a = \frac{g_{aee}}{2e}\sqrt{\frac{\hbar n_a}{m_a c}} m_a v_a$$

$$= 7 \times 10^{-23} \left(\frac{\rho_{\text{dm}}}{0.45\,\text{GeV}}\right)^{\frac{1}{2}} \left(\frac{m_a}{58.5\,\mu\text{eV}}\right) \left(\frac{v_a}{220\,\text{km/s}}\right) \text{T}$$

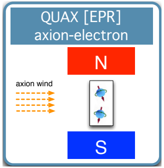

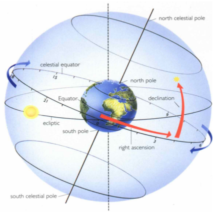

EPR/FMR technique

– material magnetized by a static magnetic field **B** $\perp$ axion wind
$\rightarrow$ DM sensing when the Larmor frequency of the electrons matches the axion frequency f_a.
– B_a deposits in the sample the power P_a
– P_a gives rise to RF/μwave radiation $\Longleftarrow$ **axion signal**

The experimental technique: electron spin resonance

Magnetic resonance (ESR/FMR) arises when energy levels of a quantized system of electronic moments are Zeeman split ($\Longleftrightarrow$ the magnetic system is placed in a uniform magnetic field B_0) and the system absorbs EM radiation in the microwave range at the Larmor frequency (ν_L).

An experimental geometry with **crossed magnetic fields** is needed:

- B_0 along $z \rightarrow \nu_L = \gamma B_0, \gamma = 28\,\mathrm{GHz/T}$
- a microwave field B_1 is applied to the xy plane
  sum of two counter-rotating fields $2A\cos\omega t = A(e^{i\omega t} + e^{-i\omega t})$
- no resonance occurs when the AC field is parallel to B_0
- $\mathbf{M} \propto n_s$ is the magnetization density

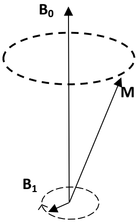

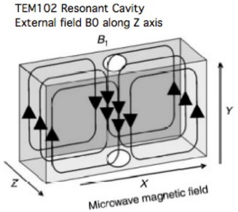

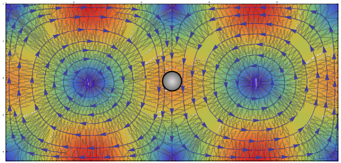

Bloch equations - spin precession

The evolution of the electron spin under the influence of external fields is described by a set of coupled non-linear equations, modified to take into account radiation damping.

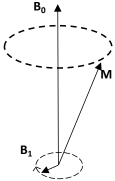

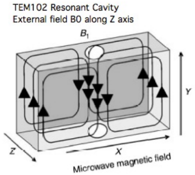

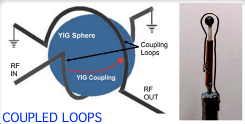

COUPLED LOOPS

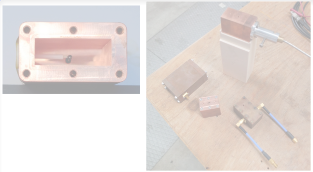

MICROWAVE CAVITY 7, 8, 12, 16 GHz rectangular cavities

MATERIAL **IN FREE SPACE**

$$
\begin{aligned}
\frac{dM_x}{dt} &= \gamma(\mathbf{M}\times\mathbf{B})_x - \frac{M_x}{\tau_2} - \frac{M_x M_z}{M_0\tau_r} \\
\frac{dM_y}{dt} &= \gamma(\mathbf{M}\times\mathbf{B})_y - \frac{M_y}{\tau_2} - \frac{M_y M_z}{M_0\tau_r} \\
\frac{dM_z}{dt} &= \gamma(\mathbf{M}\times\mathbf{B})_z - \frac{M_0 - M_z}{\tau_1} - \frac{M_x^2 + M_y^2}{M_0\tau_r}
\end{aligned}
$$

- τ_r radiation damping
- τ_1 longitudinal (spin-lattice) M_z
- $\tau_2 < \tau_1$ transverse (spin-spin) $M_{x,y}$

Axion detection via ESR

The axion wind substitutes the transverse field B1, inducing a **variable magnetization component** in the magnetic sample in the *xy* plane

$$M_a(t) = \gamma \mu_B B_a n_s \tau_{\min} \cos(\omega_a t)$$

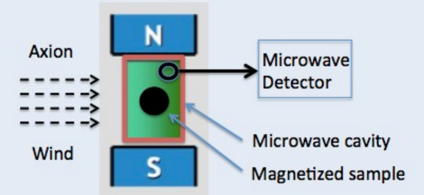

$\tau_{\min}$ is the shortest coherence time among:
— axion wind coherence time $\tau_{\nabla a}$
— magnetic material relaxation time τ_2
— radiation damping τ_r
n_s material spin density, μ_B is the Bohr magneton

Magnetized material with volume V_s will **absorb energy from the axion wind** at a rate

$$P_{\text{in}} = \mu_0 \mathbf{H} \cdot \frac{d\mathbf{M}}{dt} = B_a \frac{dM_a}{dt} V_s = \gamma \mu_B n_s \omega_a B_a^2 \tau_{\min} V_s$$

that will be re-emitted as electromagnetic radiation

Radiation damping issue

at high frequency ($\gtrsim$ 10 GHz) the signal is suppressed via τ_r term in free space ($\tau_r \ll \tau_2, \tau_{\nabla a}$)

RADIATION DAMPING AND STRONG COUPLING REGIME

- magnetized material inside a microwave cavity
- strong coupling regime: two separate resonances with width $(\tau_c^{-1} + \tau_2^{-1})$
- when the $\nu_L = \nu_c$ the system hybridizes at maximum coupling
- axion detection is accomplished in one of the *hybrid photon-magnon modes*

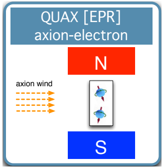

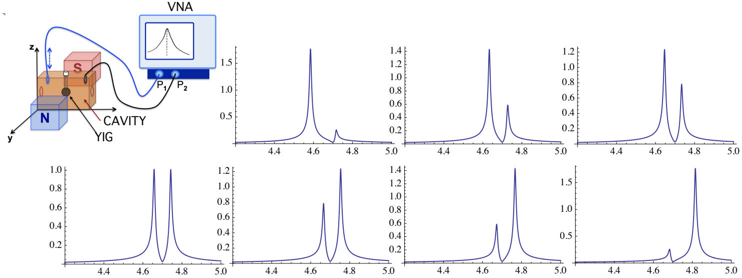

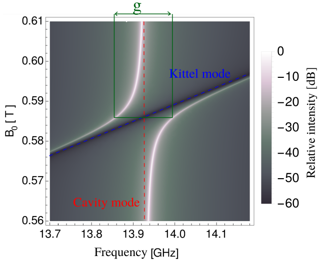

EXPECTED SIGNAL

ELECTRON COUPLING – **QUAX** NEW CONCEPT! *the FMR haloscope*

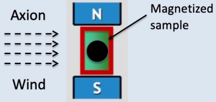

the axion DM cloud acts as an **effective RF magnetic field** on the electron spin exciting **magnetic transitions** in a magnetized sample (YIG) $\rightarrow$ **RF photons**

$$P_{\rm out} = \frac{P_{\rm in}}{2} = \mathbf{3.8\times10^{-26}} \left(\frac{m_a}{200\,\mu\text{eV}}\right)^3 \left(\frac{V_s}{100\ \text{cm}^3}\right) \left(\frac{n_S}{2\cdot10^{28}/\text{m}^3}\right) \left(\frac{\tau_{\rm min}}{2\ \mu\text{s}}\right)\ \text{W}$$

ESR (Electron Spin Resonance)
the RF field is actually the axion effective field
—>> axion mass tuning with B field!
1.7 T —> 48 GHz

YIG (Yttrium Iron Garnet)

$$\tau_{\rm min} = \min(\tau_a, \tau_c, \tau_2)$$

under the condition of **strong coupling**

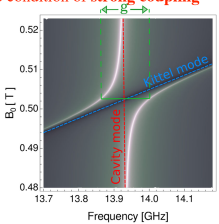

$$R_a = \frac{P_{\rm out}}{\hbar\omega_a} = \mathbf{1.2\times10^{-3}}\ \text{Hz}$$

corresponding signal photon rate
microwave photon counter is needed

EXPERIMENTAL CHALLENGES

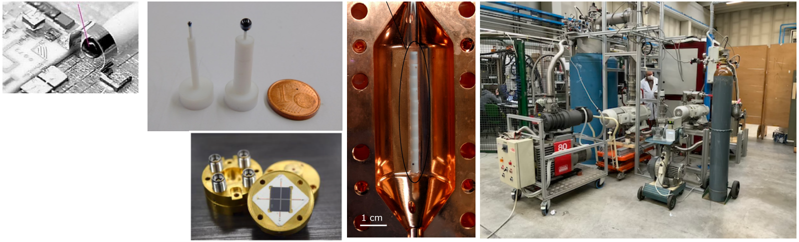

- ∘ magnetized material with spin density $2 \times 10^{28}\,\mathrm{m}^{-3}$ and FMR linewidth $\sim 150\,\mathrm{kHz}$ ($\tau_2 \sim 2\,\mu\mathrm{s}$)
- – necessary magnetized sample volume $\sim 100\,\mathrm{cm}^3$ to be hosted in $\sim 50\,\mathrm{GHz}$ frequency cavities
- • $\sim 10^6$ Q-factor cavities in multi-Tesla magnetic field
- • ppm level uniformity and high stability of the 2 T magnetic field
- – signal detection beyond SQL with linear amplifiers $\Longrightarrow$ single-photon microwave detectors
- ∘ 100 mK working temperature of the complete apparatus
- • tunability with B field

EXPERIMENTAL CHALLENGES - MAGNETIC MATERIAL

◦ magnetized material with spin density $2 \times 10^{28}\,\mathrm{m}^{-3}$ and FMR linewidth $\sim 150\,\mathrm{kHz}$ ($\tau_2 \sim 2\,\mu\mathrm{s}$)
tested several magnetic materials $\Longrightarrow$ low hybridization or too large linewidth

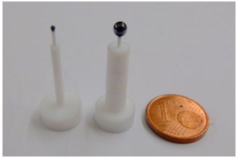

YIG – Yttrium Iron Garnet ($Y_3Fe_5O_{12}$)
— a ferrimagnetic synthetic garnet
— commercially available spheres (max 2 mm-diameter), linewidth not sufficiently narrow

We have successfully developed a procedure to get **high quality YIG spheres**:

- ⋆ acquire high purity ($\lesssim$ 1ppm RE) YIG single crystals of cm^3 size from manufacturers
- ⋆ large crystal is cut into cubes of 2.5 mm sides
- ⋆ grinding into 2 mm-diameter spheres using SiC abrasive paper of different grit size
- ⋆ polishing with Alumina based suspension

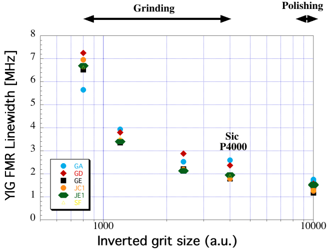

EXPERIMENTAL CHALLENGES - MAGNETIC FIELD UNIFORMITY

- Homogeneity at the ppm level is required to avoid inhomogeneous line broadening of the FMR resonance

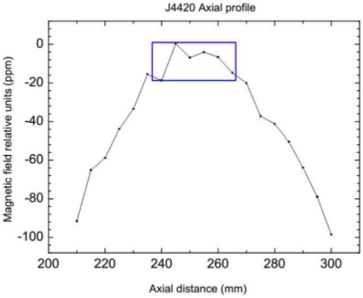

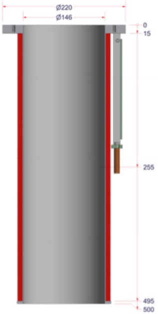

20 ppm over 1 cm, NbTi Superconducting coil
(solution from private company)

QUAX DEMONSTRATOR - 2018 LHe results

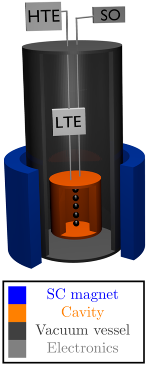

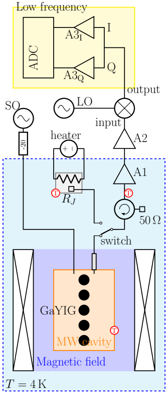

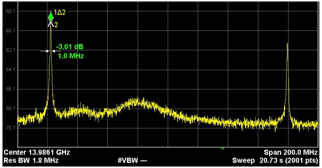

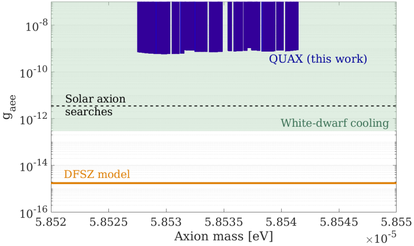

five 1-mm YIG spheres (V_s =2.6 mm^3)
HEMT low noise cryogenic amplifier $T_n = 10\,\mathrm{K}$
$T_c + T_n = 15\,\mathrm{K}$
$P_{\mathrm{in}} = (-4.6 \pm 22.2) \times 10^{-23}\ \mathrm{W}$

minimum measured value of
$g_{aee} = 4.9 \times 10^{-10} \Longleftrightarrow B_a \lesssim 2.6 \times 10^{-17}\,\mathrm{T}$
N. Crescini, et al., Eur. Phys. J. C (2018) 78:703

QUAX limit on axion-electron coupling

	QUAX 2018	QUAX 2019/2020	QUAX final
material volume	2.6 mm^3	46 mm^3	10^5 mm^3
system total noise temperature	HEMT - 15 K	JPA - 1K	**quantum counter**
relaxation time	0.1 microseconds	0.3 microseconds	2 microseconds

EPJC **78**:703 (2018)

first limit on g_{aee}

PRL **124**:171801 (2020)

- first FMR haloscope with mass scan via B
- field sensitivity 5 10^{-19}

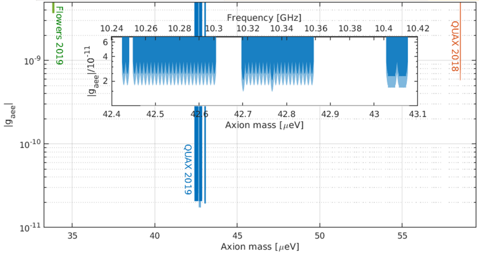

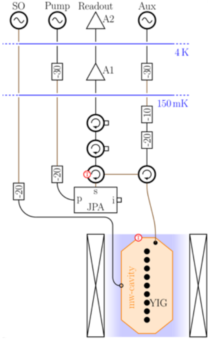

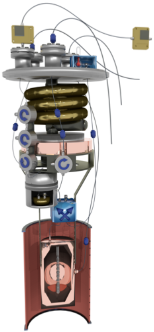

Modelling the system and frequency tuning

– new cavity at 10.7 GHz to match the JPC amplifier working frequency
– 10 spheres with max diameter 2.1 mm (selected out of about 20)

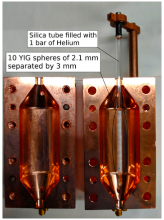

increasing the material

$\Longrightarrow$ need for *improving hybridization control*

for the FMR haloscope hybrid system
a model with 2 cavity modes + 2 magnetic modes works
$\rightarrow$ 10^{21} spins,
$\rightarrow$ coherent response by 10 spheres,
$\rightarrow$ material relaxation time 84 ns

$\rightarrow$ hybrid mode 1 is isolated, use it to search for axion-induced signals
$\rightarrow$ by changing B_0, axion mass scan along the dashed line

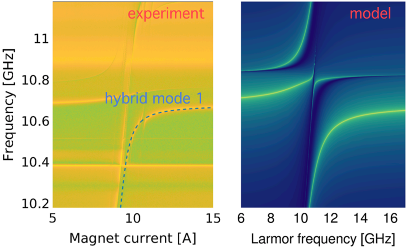

REMOVING THE MAGNETIC MATERIAL FROM THE CAVITY: QUAX a-γ

PHOTON COUPLING – QUAX aγ *high frequency range* (8.5 – 11) GHz

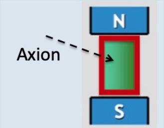

DM axions are converted into **RF photons** inside a **resonant cavity** immersed in a **strong magnetic field**

$$P_{\rm ax} = 3.3 \cdot 10^{-24}\,{\rm W} \left(\frac{V_{\rm eff}^{\rm Sa}}{2.3{\cdot}10^{-5}\,{\rm m}^3}\right)\left(\frac{B}{8\,{\rm T}}\right)^2 \times \left(\frac{g_\gamma}{-0.97}\right)^2 \left(\frac{\rho_a}{0.45\,{\rm GeV\,cm^{-3}}}\right)\left(\frac{f}{13.5\,{\rm GHz}}\right)\left(\frac{Q_L}{145\,000}\right)$$

target: high frequency range (8.5 – 11 GHz)

+ stronger magnetic field (8 T+ correction magnet to reduce stray field on electronics)
✓ high-Q cavity in intense B-fields
✓ low noise receiver, del fridge operation

Strengths:
high-Q *hybrid cavities* - NbTi sputtered on copper
dielectric resonators

High Q Dielectric cavities

normal conducting, Q_0 independent of $\mathbf{B}$

PHOTONIC CAVITY RSI **91**, 094701 (2020)

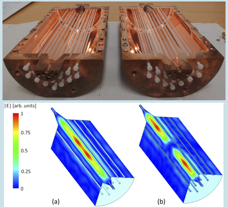

FIG. 2. Magnitude of the electric field of the first two TM resonant modes: TM010 (a) and TM011 (b).

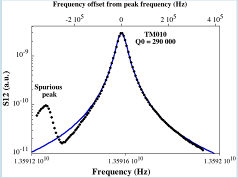

- sapphire rods
- $T = 5\,\mathrm{K}$, $Q_0 \sim 290000$
- control of rods critical

NESTED CYLINDERS NIMA **985**, 164641 (2021)

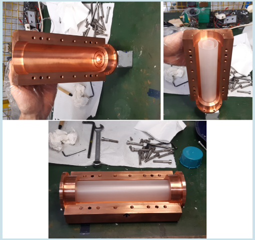

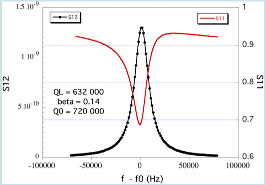

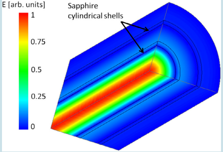

- hollow sapphire cylinders
- $T = 5\,\mathrm{K}$, $Q_0 = 720000$ (further improving...)
- cavity tuning by cyl. rotation

QUAX a-γ LIMIT ON AXION-PHOTON COUPLING

— copper cavity with conical end-caps
— two halves kept separated by lower conductivity material
— NbTi sputtering in central cylinder
(D. Alesini)

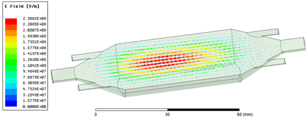

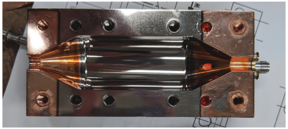

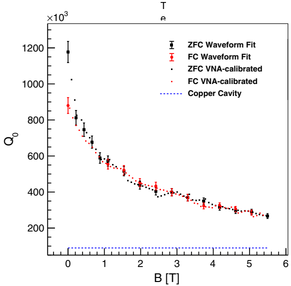

PHYS. REV. D 99, 101101 (2019)

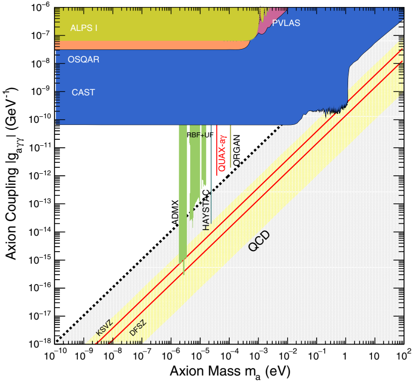

NEW! first test with JPA in 2020 reached a sensitivity of $3\times$ KSVZ in a sharp window $\rightarrow$ arXiv:2012.09498

QUAX collaboration roadmap (2021-2025)

INFN
Istituto Nazionale di Fisica Nucleare

→ DM axion search (axion-photon coupling) by scanning **yet unexplored mass values** in the $(8.5-11)$ GHz range

→ **LNL** and **LNF** INFN laboratories will work in synergy, operating in **different mass ranges** and using **different low noise amplifiers and single microwave photon detectors**.

→ strengthening collaborations with international groups for integration of

1. state-of-the-art **itinerant microwave photon counters** (E. Flurin, Saclay)
2. **traveling wave JPA** (N. Roche, Grenoble) in the receiver chain
3. high-Q cavities (SQMS, Superconducting Quantum Materials and Systems center led by Fermilab)

→ [R&D] increase the signal power in the **spin-based haloscope**. Such a detector could be crucial for the characterization of the axion models in case of discovery.

QUAX COLLABORATION ROADMAP (2021-2025)

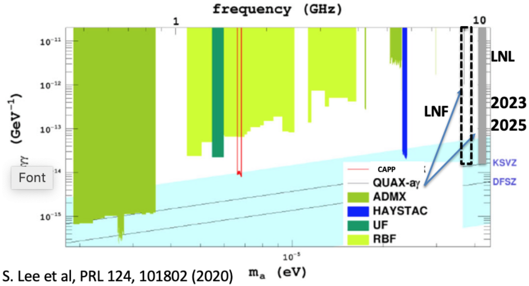

S. Lee et al, PRL 124, 101802 (2020)

Performance for KSVZ model at 95% c.l. with $N_A = 0.5$		
Noise Temperature	0.43 K	0.5 K
Single scan time	3100 s	69 s
Scan speed	18 MHz/day	40 MHz/day
Performance for KSVZ model at 95% c.l. with $N_A = 1.5$		
Noise Temperature	0.86 K	1 K
Single scan time	12500 s	280 s
Scan speed	4.5 MHz/day	10 MHz/day

	LNF	**LNL**
Magnetic field	9 T	14 T
Magnet length	40 cm	50 cm
Magnet inner diameter	9 cm	12 cm
Frequency range	8.5 - 10 GHz	9.5 - 11 GHz
Cavity type	Hybrid SC	Dielectric
Scanning type	Inserted rod	Mobile cylinder
Number of cavities	7	1
Cavity length	0.3 m	0.4 m
Cavity diameter	25.5 mm	58 mm
Cavity mode	TM010	pseudoTM030
Single volume	$1.5 \cdot 10^{-4}$ m^3	$1.5 \cdot 10^{-4}$ m^3
Total volume	7⊗0.15 liters	0.15 liters
Q_0	300 000	1 000 000
Single scan bandwidth	630 kHz	30 kHz
Axion power	$7 \otimes 1.2 \cdot 10^{-23}$ W	$0.99 \cdot 10^{-22}$ W
Preamplifier	TWJPA/INRIM	DJJAA/Grenoble
Operating temperature	30 mK	30 mK